

This article was downloaded by: [LSE Library]

On: 18 March 2013, At: 13:36

Publisher: Taylor & Francis

Informa Ltd Registered in England and Wales Registered Number: 1072954 Registered office: Mortimer House, 37-41 Mortimer Street, London W1T 3JH, UK



## Journal of the American Statistical Association

Publication details, including instructions for authors and subscription information:

<http://www.tandfonline.com/loi/uasa20>

### Modeling and Forecasting Daily Electricity Load Curves: A Hybrid Approach

Haeran Cho <sup>a</sup>, Yannig Goude <sup>b</sup>, Xavier Brossat <sup>b</sup> & Qiwei Yao <sup>c d</sup>

<sup>a</sup> Department of Statistics, London School of Economics, UK

<sup>b</sup> Electricité de France, R&D, Clamart, France

<sup>c</sup> Department of Statistics, London School of Economics, Houghton Street, London, WC2A 2AE, U.K.

<sup>d</sup> Guanghua School of Management, Peking University, China

Accepted author version posted online: 12 Sep 2012. Version of record first published: 15 Mar 2013.

To cite this article: Haeran Cho, Yannig Goude, Xavier Brossat & Qiwei Yao (2013): Modeling and Forecasting Daily Electricity Load Curves: A Hybrid Approach, Journal of the American Statistical Association, 108:501, 7-21

To link to this article: <http://dx.doi.org/10.1080/01621459.2012.722900>

PLEASE SCROLL DOWN FOR ARTICLE

Full terms and conditions of use: <http://www.tandfonline.com/page/terms-and-conditions>

This article may be used for research, teaching, and private study purposes. Any substantial or systematic reproduction, redistribution, reselling, loan, sub-licensing, systematic supply, or distribution in any form to anyone is expressly forbidden.

The publisher does not give any warranty express or implied or make any representation that the contents will be complete or accurate or up to date. The accuracy of any instructions, formulae, and drug doses should be independently verified with primary sources. The publisher shall not be liable for any loss, actions, claims, proceedings, demand, or costs or damages whatsoever or howsoever caused arising directly or indirectly in connection with or arising out of the use of this material.

# Modeling and Forecasting Daily Electricity Load Curves: A Hybrid Approach

Haeran CHO, Yannig GOUDE, Xavier BROSSAT, and Qiwei YAO

We propose a hybrid approach for the modeling and the short-term forecasting of electricity loads. Two building blocks of our approach are (1) modeling the overall trend and seasonality by fitting a generalized additive model to the *weekly* averages of the load and (2) modeling the dependence structure across consecutive *daily* loads via curve linear regression. For the latter, a new methodology is proposed for linear regression with both curve response and curve regressors. The key idea behind the proposed methodology is dimension reduction based on a singular value decomposition in a Hilbert space, which reduces the curve regression problem to several ordinary (i.e., scalar) linear regression problems. We illustrate the hybrid method using French electricity loads between 1996 and 2009, on which we also compare our method with other available models including the Électricité de France operational model. Supplementary materials for this article are available online.

KEY WORDS: Correlation dimension; Dimension reduction; Electricity loads; Generalized additive models; Singular value decomposition.

## 1. INTRODUCTION

As electricity can be stored or discharged only at extra costs, it is an important task for electricity providers to model and forecast electricity loads accurately over short-term (from one-day to one-month ahead) or middle-term (from one-month to five-year ahead) horizons. The electricity load forecast is an essential component of the optimization tools adopted by energy companies for power system scheduling. A small improvement in load forecasting can bring substantial benefits by reducing production costs as well as increasing trading advantages, especially during peak periods.

The French energy company Électricité de France (EDF) manages a large panel of production units in France and in Europe, which include water dams, nuclear plants, wind turbines, and coal and gas plants. Over the years, EDF has developed a very accurate load forecasting model that consists of complex regression methods coupled with classical time series techniques such as the seasonal autoregressive integrated moving average (SARIMA) model. The model integrates a great deal of physical knowledge of French electricity consumption patterns that has been accumulated over 20 years, such as the fact that the temperature felt indoors is more relevant than the real temperature in modeling the electricity load. Furthermore, it includes exogenous information ranging from economic growth forecasts to different tariff options provided by EDF. The forecasting model in operation performs very well at present, attaining about 1% mean absolute percentage error (MAPE) in forecasting over the one-day horizon. However, it has a drawback in terms of its poor capacity in adapting to changes in electricity consumption habits, which may occur due to the opening of new electricity markets, technological innovations, social and economic changes, to name a few. Hence, it is strategically important to

develop some new forecasting models that are more adaptive to an ever-changing electricity consumption environment, and the hybrid method proposed in this article, designed for short-term forecasting for daily loads, represents a determined effort in this direction.

Electricity load exhibits interesting features at different levels. Figure 1 displays the electricity load in France measured every half an hour from 1996 to 2009. First of all, there is an overall increasing trend due to meteorological and economic factors. In addition, a seasonal pattern repeats itself every year that can be explained by seasonal changes in temperature, day light duration, and cloud cover. Engle et al. (1986) and Taylor and Buizza (2002) discussed the impact of meteorological factors on the electricity load, and singled out the temperature as being the most important due to the large demand of electrical heating in cold weather. Further studies on the meteorological effect include Taylor and McSharry (2008), where seasonal patterns of electricity loads over 10 European countries were reported. Also, there exist daily patterns that, unfortunately, do not show up due to the large scale of Figure 1, attributed to varying demands for electricity within a day. Figure 6 provides an example of such daily patterns.

Based on the above observations, we propose to model electricity loads at two different levels using different methods, hence the name *hybrid* approach. First, assuming that the long-term trends do not vary greatly within a week, we extract those trends from weekly average loads using a generalized additive model (GAM), where temperature and other meteorological factors are included as additional explanatory variables. After removing the long-term trend component from the data, we view the daily loads as curves and model the dynamic dependence among the electricity loads of successive days via curve linear regression. For this, a new dimension-reduction technique based on a singular value decomposition (SVD) in Hilbert space is proposed, which reduces the regression with a curve response and a curve regressor to several ordinary (i.e., scalar) linear

Haeran Cho is Postdoctoral research officer, Department of Statistics, London School of Economics, UK (E-mail: [h.cho1@lse.ac.uk](mailto:h.cho1@lse.ac.uk)). Yannig Goude (E-mail: [yannig.goude@edf.fr](mailto:yannig.goude@edf.fr)) and Xavier Brossat (E-mail: [xavier.brossat@edf.fr](mailto:xavier.brossat@edf.fr)) are at Electricité de France, R&D, Clamart, France. Qiwei Yao is Professor, Department of Statistics, London School of Economics, Houghton Street, London, WC2A 2AE, U.K.; Guanghua School of Management, Peking University, China (E-mail: [q.yao@lse.ac.uk](mailto:q.yao@lse.ac.uk)). Partially supported by the EPSRC research grant EP/G026874/1.

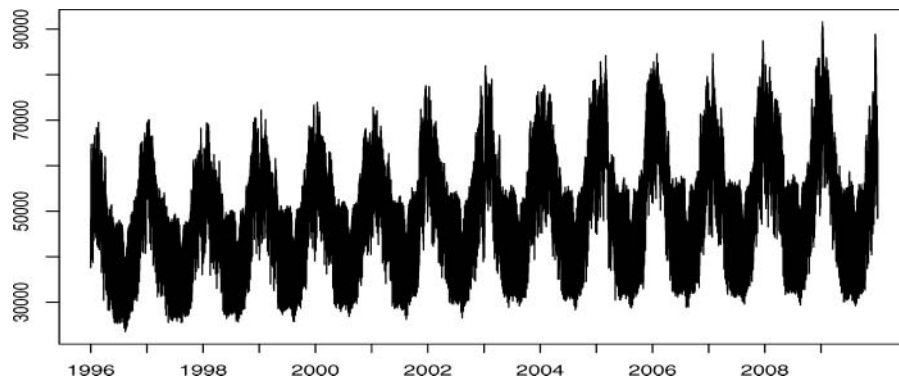


Figure 1. Electricity load from 1996 to 2009 in France.

regression models. Regarding the daily loads as curves, our approach takes advantage of the continuity of the consumption curves in statistical modeling, as well as embedding some nonstationary features (such as daily patterns) into a stationary framework in a functional space.

When applied to electricity load forecasting, the proposed method is shown to provide more accurate predictions than conventional methods such as those based on SARIMA models or exponential smoothing. Although the operational model at EDF provides more accurate predictions than our method, the latter is considerably simpler and does not make use of the full subject knowledge that has been accumulated over more than 20 years at the EDF, which is not available in the public domain. Hence, our approach is more adaptive to the changing electricity consumption environment while retaining a competitive prediction capacity, and can be adopted as a generic tool applicable to a wide range of problems including electricity load forecasting in countries other than France. Furthermore, it has the potential to serve as a building block for constructing a more effective operational model when incorporating the full EDF subject knowledge.

There is a growing body of literature devoted to electricity load forecasting models. Focusing on the main interest of this article, we list below the recent articles on short-term load forecasting; see Bunn and Farmer (1985) for a more comprehensive overview. In the category of parametric approaches, Ramanathan et al. (1997) proposed linear regression models with autoregressive errors for each hour of a day. Univariate methods such as those based on SARIMA models or exponential smoothing can be found in Hyndman et al. (2002), Taylor, de Menezes, and McSharry (2006), and Taylor (2010), and those based on state-space models in Dordonnat et al. (2008) and Dordonnat et al. (2011). Among the nonparametric and semiparametric methods, Engle et al. (1986) proposed to include the temperature effect in the load modeling, and Harvey and Koopman (1993) proposed a time-varying spline model that captured both the temperature effect and the seasonal patterns in a semiparametric way. GAMs for electricity loads were studied in Pierrot and Goude (2011) and Fan and Hyndman (2012), where the semiparametric approaches were shown to be well adapted to nonlinear behaviors of the electricity load signal. In Antoniadis, Paparoditis, and Sapatinas (2006), a forecasting model based on functional data analysis was proposed, which treated the daily electricity loads as curves, and the approach has been further developed in Cugliari (2011). Cottet and Smith

(2003) proposed a Bayesian autoregressive model for short-term forecasts, where the meteorological effects were estimated as nonlinear using semiparametric regression methods. They obtained good forecasting results with New South Wales dataset.

The rest of the article is organized as follows. In Section 2, we present the modeling of weekly average loads using a GAM. Then Section 3 discusses the modeling of the dependence structure between daily loads in a curve linear regression framework. We conduct a comparison study in Section 4, where our new method as well as other competitors are applied to predict the French daily loads in 2009. Section 5 contains some conclusive remarks. All the proofs are relegated to an online supplementary document.

## 2. MODELING WEEKLY AVERAGES

Assuming that the overall trend and seasonality do not vary greatly within a week, we propose to model the long-term trends with the *weekly* averages, that is, we treat the trend and seasonal component as being constant within each week. In this manner, we lose little from the gradual changes of the trends within each week, while preserving the dependence structure across the electricity loads of different days. The weekly averages of the EDF loads from 1996 to 2008 are plotted in Figure 2. In the literature, it has been noted that some meteorological factors, such as temperature and cloud cover, have a significant impact on electricity consumption patterns. While there are other detrending techniques that have been proposed for removing long-term trends and seasonal cycles, we fit the weekly averages using a GAM for its ability to model implicit nonlinear relationships between response and explanatory variables without suffering from the so-called “curse of dimensionality”; see Hastie and Tibshirani (1990) and Wood (2006) for further details on the GAM, and Pierrot, Lahuque, and Goude (2009), Pierrot and Goude (2011), and Fan and Hyndman (2012) for its application to electricity load modeling. Denoting the time index representing each week by  $t$ , the explanatory variables considered in fitting the weekly average load process  $L_t$  are as follows:  $O_t$  is the weekly median of the *offset* (a temporal variable determined by the experts at EDF to represent the seasonal trend in the data, taking values  $-3, -2, -1$ , and  $0$  to denote different winter holidays,  $1$  to denote spring,  $2-6$  to denote summer and summer holidays, and  $7$  to denote autumn),  $T_t$  is the weekly average of the temperature,  $C_t$  is the weekly average of the cloud cover, and  $I_t$  is the weekly index ranging from 1 to 53.

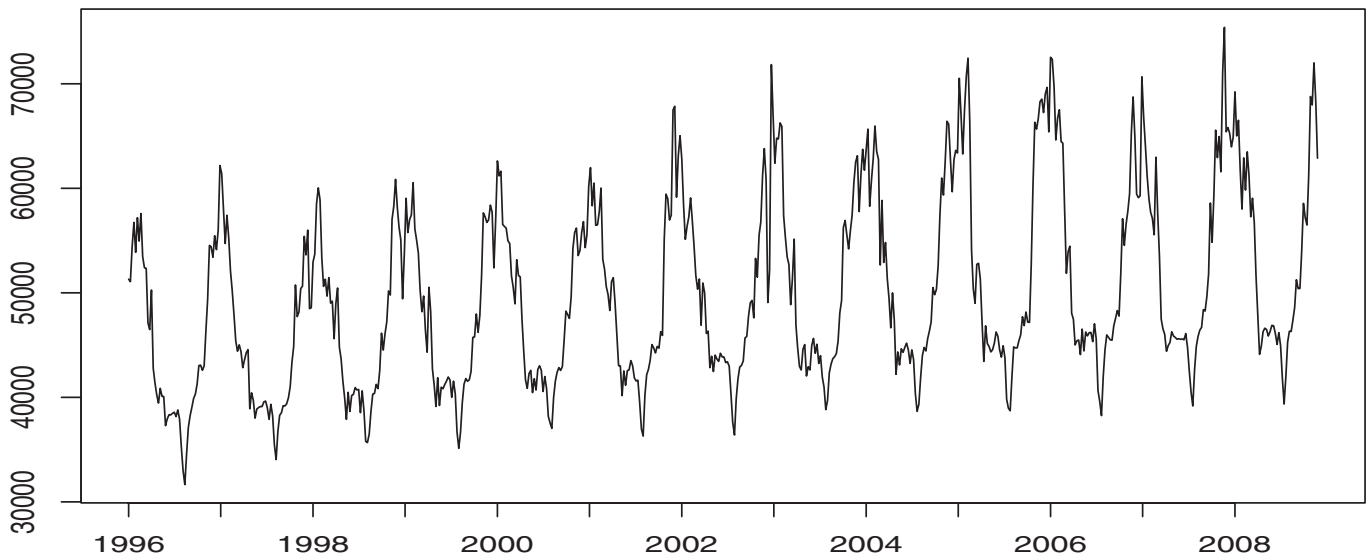


Figure 2. Weekly average electricity load in France from 1996 to 2008.

Our first attempt at taking into account the meteorological effects as well as the temporal trend is summarized in the following GAM with the Gaussian link function

$$L_t = f_1(t) + f_2(O_t) + f_3(L_{t-1}) + f_4(T_t) + f_5(T_{t-1}) + f_6(C_t), \quad (1)$$

where each  $f_j$  is a smooth function of the corresponding covariate with thin plate regression splines as a smoothing basis. We use the R package *mgcv* introduced in Wood (2006), where each smooth function  $f_j$  is estimated by penalized regression splines. In this implementation, the amount of penalization is calibrated according to the generalized cross-validation (GCV) score, see Wood (2004, 2011) for details.

We note that the basis used to estimate  $f_1$  has knots at each first week of September, which are imposed to model the time-varying trend in the electricity load at the yearly level. The

boxplot of the residuals from fitting the above GAM to the weekly average load between 1996 and 2008 is provided in Figure 3, and the estimated curves for  $f_1, \dots, f_6$  in (1) are plotted in Figure 4, with shaded area representing the twice standard error bands below and above the estimate. The fitted curve explains 98.7% of the data, and the MAPE and the root mean square error (RMSE) from the estimated curve are 1.63% and 1014 MW, respectively. The two error measures, MAPE and RMSE, are defined as

$$\begin{aligned} \text{MAPE} &= \frac{1}{T} \sum_{t=1}^T \left| \frac{\hat{L}_t - L_t}{L_t} \right| \quad \text{and} \\ \text{RMSE} &= \left\{ \frac{1}{T} \sum_{t=1}^T (\hat{L}_t - L_t)^2 \right\}^{1/2}, \end{aligned} \quad (2)$$

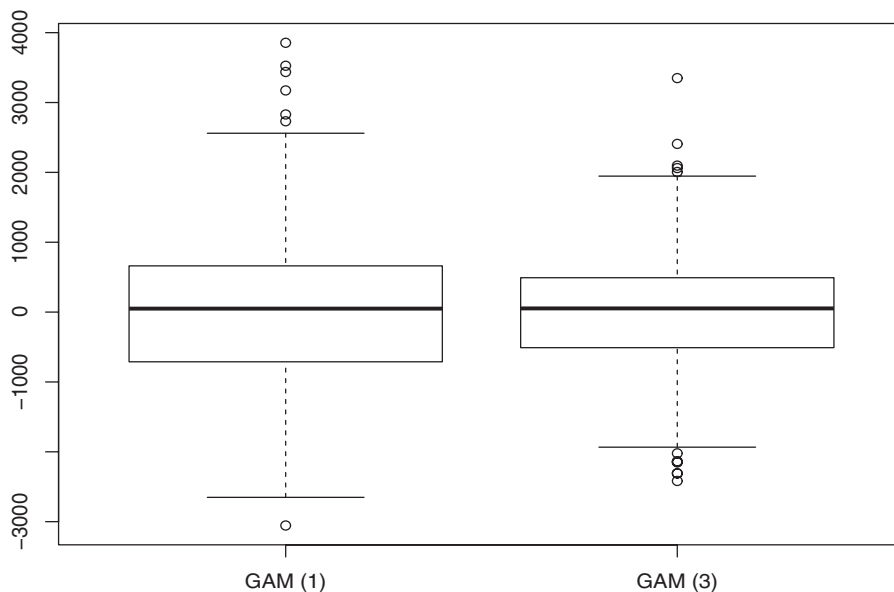


Figure 3. Boxplots of the residuals from fitting the weekly average load between 1996 and 2008 using the model (1) (left) and the model (3) (right).

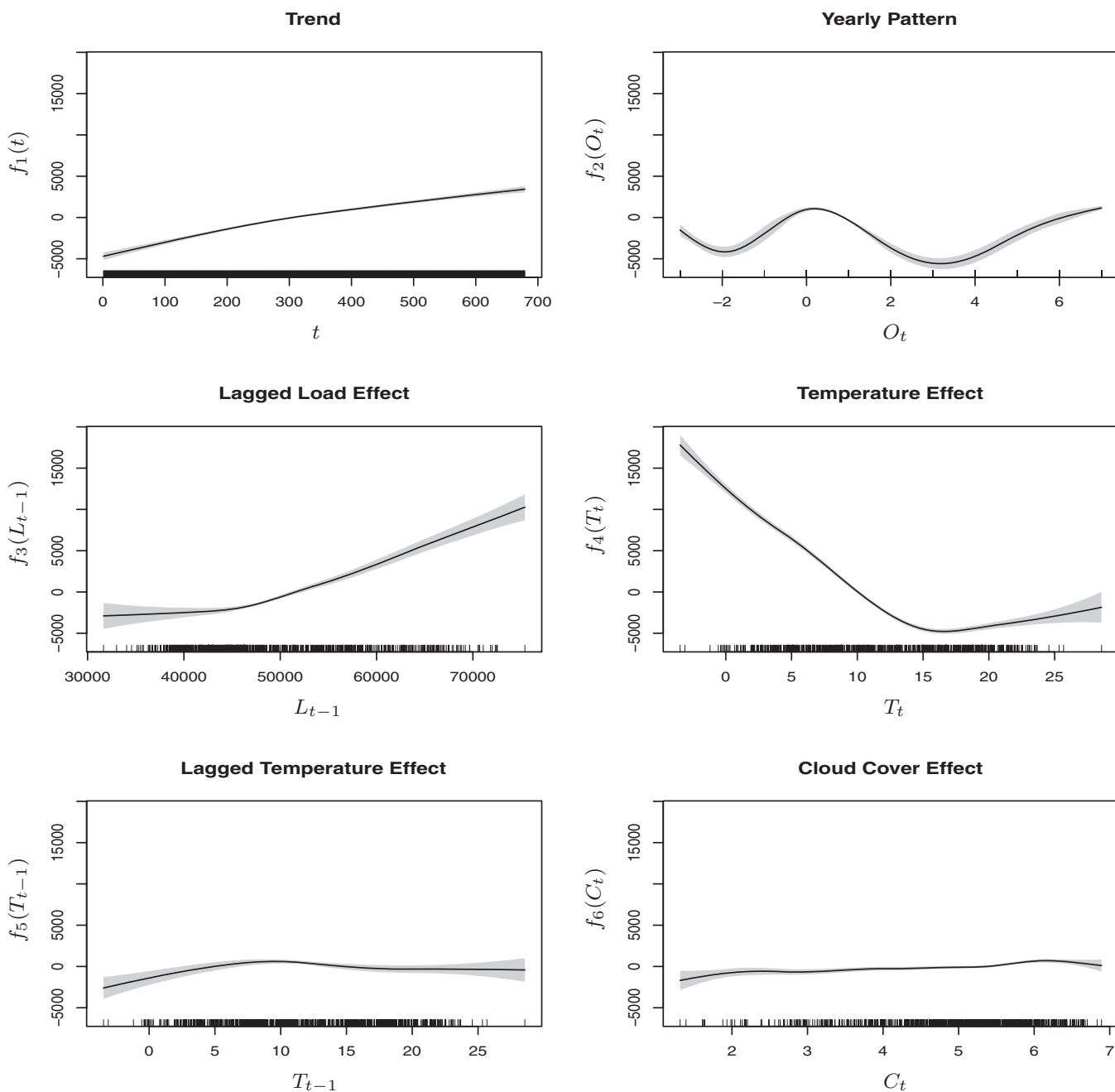


Figure 4. Estimated  $f_1, \dots, f_6$  from model (1); shaded regions represent the confidence bands.

where  $\hat{L}_t$  denotes the estimated (or predicted) load in the week  $t$ .

We state below some observations based on the estimated functions in Figure 4. The top left panel shows that the electricity load increases over time  $t$ , and that the trend is almost linear. The top right panel shows clearly the presence of seasonality as the load is lower during holidays and in summer than in winter. As for the lagged load effect,  $L_t$  increases with respect to its lagged value  $L_{t-1}$  (the second left panel) and the rate of increase is greater when  $L_{t-1} > 5 \times 10^4$  approximately, which implies that the value  $5 \times 10^4$  may be regarded as a “threshold” acting on the impact of  $L_{t-1}$  on  $L_t$ . Since the increase in the usage of electricity is closely related to the climate, which in turn is linked to the time of the year, we may include the joint effect

of  $L_{t-1}$  and  $I_t$  in the model to accommodate the dependence between those two variables. Also, the impact of temperature is significant (the second right panel). Low temperatures lead to high electricity consumption due to electrical heating, resulting in the initial sharp decrease in  $\hat{f}_4$ . Then as the temperature increases from about 17°C upward,  $\hat{f}_4$  also increases slowly, which can be accounted for by the use of cooling systems in hot weather. As the meteorological changes within a year are closely related to the time index, we may include the joint effect of the variables  $T_t$  and  $I_t$  in the model. The bottom panels show that, although not as prominent as other terms, the lagged temperature and the cloud cover do have an impact on the weekly average load at large values of  $T_{t-1}$  and  $C_t$ . The effect of cloud cover is significantly different from 0 for large values of  $C_t$ , as heavy

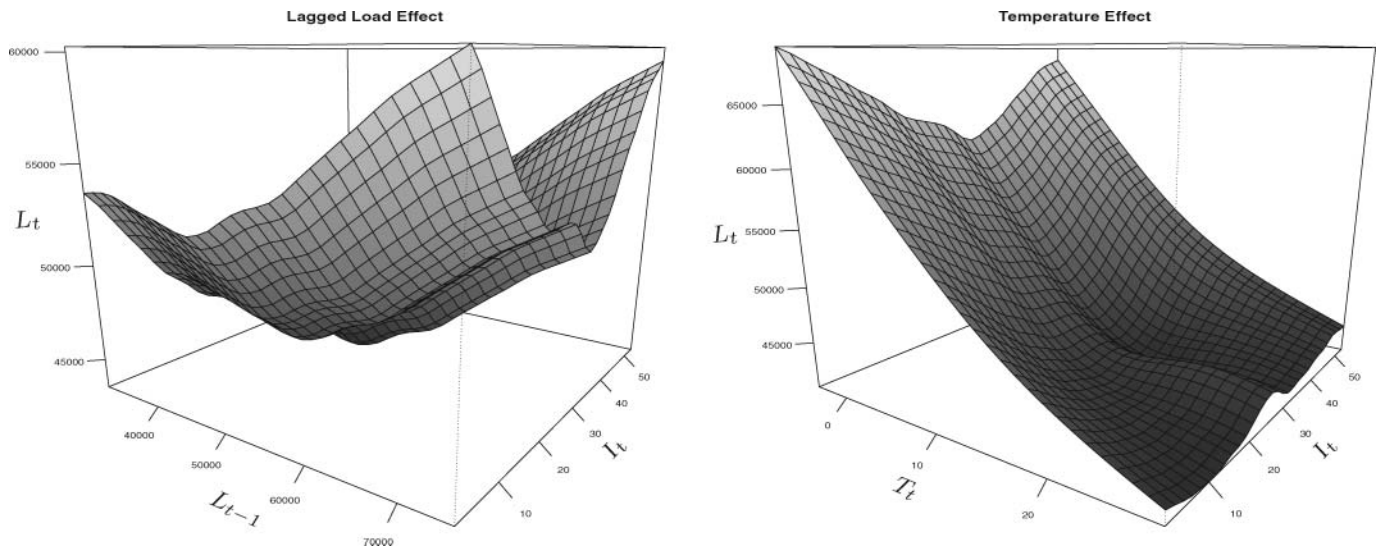


Figure 5. Estimated  $f_3$  (left) and  $f_4$  (right) from model (3).

cloud cover induces the increasing use of lighting (the bottom right panel). We note that the estimated effect of low cloud cover may be an artifact: there are only few observations available for low cloud cover and thus the variance of the fitted curve at such small values of  $C_t$  is large.

Based on the above observations, we propose another model

$$L_t = f_1(t) + f_2(O_t) + f_3(L_{t-1}, I_t) + f_4(T_t, I_t) + f_5(T_{t-1}, I_t) + f_6(C_t, I_t), \quad (3)$$

where  $f_3, \dots, f_6$  include the weekly index  $I_t$  as a covariate. To study the bivariate effects, the estimated  $f_3$  and  $f_4$  are plotted in Figure 5. The impact of the lagged load  $L_{t-1}$  on the load  $L_t$  is similar as previously described in the sense that the rate of increase of  $L_t$  changes when  $L_{t-1}$  is greater than a threshold value. However, we also note that the relationship between  $L_{t-1}$  and  $L_t$  varies throughout a year with the weekly index  $I_t$ , and that the impact of  $L_{t-1}$  is far stronger in winter than in summer. As for the effect of temperature, there is a smooth transition observable throughout a year from the winter heating effect to the summer cooling effect.

With the new model, there is an increase in the percentage of the data explained (99.2%), and both the MAPE (1.28%) and the RMSE (801 MW) of the fitted trend have decreased. Further, the GCV score indicates that the new model is favored ( $8.4 \times 10^5$ ) over the previous one ( $1.2 \times 10^6$ ). Also, when comparing the forecasts from the two models for the weekly average loads of 2009, model (3) performed considerably better (MAPE 1.72%, RMSE 1250 MW) than model (1) (MAPE 2.15%, RMSE 1532 MW). We note that the superior performance of the model (3) at the weekly level carries over to that at the daily electricity load forecasting; when applied to forecast the daily loads in 2009, the MAPE and RMSE from the model (3) were 1.35% and 869 MW, respectively, whereas the model (1) led to 1.41% and 901 MW (see Section 4 for full details of the forecasting procedure). From these observations and also from the residual boxplots in Figure 3, we choose model (3) over model (1).

### 3. REGRESSION OF DAILY LOAD CURVES

Once the long-term trend is fitted as in Section 2 and removed, we regard the residuals on the  $i$ th day as a curve  $Y_i(\cdot)$  defined on the index set  $\mathcal{I}_1$ , and model the dependency among the daily loads via curve linear regression as

$$Y_i(u) = \int_{\mathcal{I}_2} X_i(v)\beta(u, v)dv + \varepsilon_i(u) \quad \text{for } u \in \mathcal{I}_1, \quad (4)$$

where  $X_i(\cdot)$  can be, for example, the residual curve on the  $(i-1)$ th day (i.e.,  $Y_{i-1}(\cdot)$ ), or the curve joining  $Y_{i-1}(\cdot)$  and the temperature curve on the  $i$ th day. Therefore, the index set of  $X_i(\cdot)$ , say  $\mathcal{I}_2$ , may be different from  $\mathcal{I}_1$ . In (4),  $\beta$  is a regression coefficient function defined on  $\mathcal{I}_1 \times \mathcal{I}_2$ , and  $\varepsilon_i(\cdot)$  is noise with mean 0.

Linear regression with curves as both response and regressor has been studied by Ramsay and Dalzell (1991), He, Müller, and Wang (2000), Chiou, Müller, and Wang (2004), and Yao, Müller, and Wang (2005) among others. The conventional approach is to apply the Karhunen–Loève decomposition to both  $Y_i(\cdot)$  and  $X_i(\cdot)$ , and then to fit a regression model using the finite number of terms obtained from such decompositions. The Karhunen–Loève decomposition has featured predominantly in functional data analysis; see also Fan and Zhang (1998) and Hall and Horowitz (2007). This approach is identical to dimension reduction based on principal component analysis in multivariate analysis. Since the principal components do not necessarily represent the directions in which  $X_i(\cdot)$  and  $Y_i(\cdot)$  are most correlated, we present below a novel approach where the SVD is applied to single out the directions upon which the projections of  $Y_i(\cdot)$  are most correlated with  $X_i(\cdot)$ . Our method is closely related to canonical correlation analysis yet we focus on regressing  $Y_i(\cdot)$  on  $X_i(\cdot)$ , and thus  $Y_i(\cdot)$  and  $X_i(\cdot)$  are not treated on an equal footing, which is different from, and much simpler than, the canonical correlation analysis. The literature on functional canonical correlation analysis includes Hannan (1961), Silverman (1996), He, Müller, and Wang (2003), Cupidon et al. (2008), Eubank and Hsing (2008), and Yang, Müller, and Stadtmüller (2011).

### 3.1 Curve Linear Regression via Dimension Reduction

Let  $\{Y_i(\cdot), X_i(\cdot)\}$ ,  $i = 1, \dots, n$ , be a random sample where  $Y_i(\cdot) \in \mathcal{L}_2(\mathcal{I}_1)$ ,  $X_i(\cdot) \in \mathcal{L}_2(\mathcal{I}_2)$ , and let  $\mathcal{I}_1$  and  $\mathcal{I}_2$  be two compact subsets of  $\mathbb{R}$ . We denote by  $\mathcal{L}_2(\mathcal{I})$  the Hilbert space consisting of all the square integrable curves defined on the set  $\mathcal{I}$ , which is equipped with the inner product  $\langle f, g \rangle = \int_{\mathcal{I}} f(u)g(u)du$  for any  $f, g \in \mathcal{L}_2(\mathcal{I})$ . We assume that  $\mathbb{E}\{Y_i(u)\} = 0$  for all  $u \in \mathcal{I}_1$  and  $\mathbb{E}\{X_i(v)\} = 0$  for all  $v \in \mathcal{I}_2$ , and denote the covariance function between  $Y_i(\cdot)$  and  $X_i(\cdot)$  by  $\Sigma(u, v) = \text{cov}\{Y_i(u), X_i(v)\}$ . Under the assumption

$$\int_{\mathcal{I}_1} \mathbb{E}\{Y_i(u)^2\}du + \int_{\mathcal{I}_2} \mathbb{E}\{X_i(v)^2\}dv < \infty, \quad (5)$$

$\Sigma$  defines the following two bounded operators between  $\mathcal{L}_2(\mathcal{I}_1)$  and  $\mathcal{L}_2(\mathcal{I}_2)$ :

$$\begin{aligned} f_1(u) &\rightarrow \int_{\mathcal{I}_1} \Sigma(u, v)f_1(u)du \in \mathcal{L}_2(\mathcal{I}_2), \\ f_2(v) &\rightarrow \int_{\mathcal{I}_2} \Sigma(u, v)f_2(v)dv \in \mathcal{L}_2(\mathcal{I}_1) \end{aligned}$$

for any  $f_i \in \mathcal{L}_2(\mathcal{I}_i)$ . Based on the SVD, there exists a triple sequence  $\{(\varphi_j, \psi_j, \lambda_j), j = 1, 2, \dots\}$  for which

$$\Sigma(u, v) = \sum_{j=1}^{\infty} \sqrt{\lambda_j} \varphi_j(u) \psi_j(v), \quad (6)$$

where  $\{\varphi_j\}$  is an orthonormal basis of  $\mathcal{L}_2(\mathcal{I}_1)$ ,  $\{\psi_j\}$  is an orthonormal basis of  $\mathcal{L}_2(\mathcal{I}_2)$ , and  $\{\lambda_j\}$  are ordered such that

$$\lambda_1 \geq \lambda_2 \geq \dots \geq 0. \quad (7)$$

Further, it holds that for  $u \in \mathcal{I}_1$ ,  $v \in \mathcal{I}_2$  and  $j = 1, 2, \dots$ ,

$$\begin{aligned} \int_{\mathcal{I}_1} M_1(u, z) \varphi_j(z) dz &= \lambda_j \varphi_j(u), \\ \int_{\mathcal{I}_2} M_2(v, z) \psi_j(z) dz &= \lambda_j \psi_j(v), \end{aligned} \quad (8)$$

where  $M_i$  is a nonnegative operator defined on  $\mathcal{L}_2(\mathcal{I}_i)$  as

$$\begin{aligned} M_1(u, u') &= \int_{\mathcal{I}_2} \Sigma(u, z) \Sigma(u', z) dz, \\ M_2(v, v') &= \int_{\mathcal{I}_1} \Sigma(z, v) \Sigma(z, v') dz. \end{aligned}$$

It is clear from (8) that  $\lambda_j$  is the  $j$ th largest eigenvalue of  $M_1$  and  $M_2$  with  $\varphi_j$  and  $\psi_j$  as the corresponding eigenfunctions, respectively. Since  $\{\varphi_j\}$  and  $\{\psi_j\}$  are the orthonormal basis of  $\mathcal{L}_2(\mathcal{I}_1)$  and  $\mathcal{L}_2(\mathcal{I}_2)$ , we may write

$$Y_i(u) = \sum_{j=1}^{\infty} \xi_{ij} \varphi_j(u), \quad X_i(v) = \sum_{j=1}^{\infty} \eta_{ij} \psi_j(v), \quad (9)$$

where  $\xi_{ij}$  and  $\eta_{ij}$  are random variables defined as

$$\xi_{ij} = \int_{\mathcal{I}_1} Y_i(u) \varphi_j(u) du, \quad \eta_{ij} = \int_{\mathcal{I}_2} X_i(v) \psi_j(v) dv. \quad (10)$$

It follows from (6) that

$$\text{cov}(\xi_{ij}, \eta_{ik}) = \mathbb{E}(\xi_{ij} \eta_{ik}) = \begin{cases} \sqrt{\lambda_j} & \text{for } j = k, \\ 0 & \text{for } j \neq k. \end{cases} \quad (11)$$

We refer to Smithies (1937) for further details on the SVD in a Hilbert space.

Now, we are ready to introduce the notion of the correlation dimension between the two curves. See Hall and Vial (2006) and Bathia, Yao, and Ziegelmann (2010) for the definitions of curve dimensionality in different contexts.

*Definition 1.* The correlation between curves  $Y_i(\cdot)$  and  $X_i(\cdot)$  is  $r$ -dimensional if  $\lambda_r > 0$  and  $\lambda_{r+1} = 0$  in (7).

When the correlation between  $Y_i(\cdot)$  and  $X_i(\cdot)$  is  $r$ -dimensional, it follows from (11) that  $\text{cov}\{\xi_{ij}, X_i(v)\} = 0$  for all  $j > r$  and  $v \in \mathcal{I}_2$ . Moreover, the curve linear regression model (4) admits an equivalent representation with  $r$  (scalar) linear regression models; see Theorem 1. Before presenting the theorem, we further assume that the regression coefficient  $\beta(u, v)$  is in the Hilbert space  $\mathcal{L}_2(\mathcal{I}_1 \times \mathcal{I}_2)$ , and that  $\varepsilon_i(\cdot)$  are iid with  $\mathbb{E}\{\varepsilon_i(u)\} = 0$  and  $\mathbb{E}\{X_i(v)\varepsilon_j(u)\} = 0$  for any  $u \in \mathcal{I}_1$ ,  $v \in \mathcal{I}_2$ , and  $i, j \geq 1$ .

*Theorem 1.* Let the linear correlation between  $Y_i(\cdot)$  and  $X_i(\cdot)$  be  $r$ -dimensional. Then the curve regression (4) may be represented equivalently by

$$\begin{aligned} \xi_{ij} &= \sum_{k=1}^{\infty} \beta_{jk} \eta_{ik} + \varepsilon_{ij} & \text{for } j = 1, \dots, r, \\ \xi_{ij} &= \varepsilon_{ij} & \text{for } j = r + 1, r + 2, \dots, \end{aligned} \quad (12)$$

where  $\varepsilon_{ij} = \int_{\mathcal{I}_1} \varphi_j(u) \varepsilon_i(u) du$  and  $\beta_{jk} = \int_{\mathcal{I}_1 \times \mathcal{I}_2} \varphi_j(u) \psi_k(v) \beta(u, v) dudv$ .

The proof of Theorem 1 can be found in the supplementary document. Some remarks are listed in order.

- (a) For each  $j = 1, \dots, r$ , we may apply model selection criteria such as the Akaike information criterion, to select the variables to be included in the first linear regression model of (12) among  $\{\eta_{ik}, k \geq 1\}$ , noting  $\text{var}(\eta_{ik}) \rightarrow 0$  as  $k \rightarrow \infty$ ; see (5) and (9). We also note that  $\{\varphi_j(u) \psi_k(v)\}_{j,k}$  form an orthonormal basis of  $\mathcal{L}_2(\mathcal{I}_1 \times \mathcal{I}_2)$ . Since  $\beta(u, v) \in \mathcal{L}_2(\mathcal{I}_1 \times \mathcal{I}_2)$ , it holds that  $\sum_{j=1}^{\infty} \sum_{k=1}^{\infty} \beta_{jk}^2 = \int_{\mathcal{I}_1 \times \mathcal{I}_2} \beta(u, v)^2 dudv < \infty$ .
- (b) In fact, Theorem 1 holds for any valid expansion of  $X_i(v)$  as  $X_i(v) = \sum_k \eta_{ik} \psi_k(v)$ , provided  $\{\xi_{ij}\}$  are obtained from the SVD. For example, we may use the Karhunen–Loève decomposition of  $X_i(\cdot)$ . Then resulting  $\eta_{ik}$  is the projection of  $X_i(\cdot)$  on the  $k$ th principal direction, and those  $\{\eta_{ik}\}$  are uncorrelated with each other.
- (c) Let  $X_i(\cdot)$  be of finite dimension in the sense that its Karhunen–Loève decomposition has  $q$  terms only as  $X_i(v) = \sum_{k=1}^q \zeta_{ik} \gamma_k(v)$ , where  $q (\geq r)$  is a finite integer,  $\{\gamma_k(\cdot)\}_{k=1}^q$  are  $q$  orthonormal functions in  $\mathcal{L}_2(\mathcal{I}_2)$ , and  $\zeta_{i1}, \dots, \zeta_{iq}$  are uncorrelated with  $\text{var}(\zeta_{ik}) > 0$  for all  $k = 1, \dots, q$ . Without loss of generality, we may assume that  $\text{var}(\zeta_{ik}) = 1$ , which can be achieved by replacing  $X_i(v)$  with its linear transformation  $\int_{\mathcal{I}_2} \Gamma(v, w) X_i(w) dw$ , where  $\Gamma(v, w) = \sum_{k=1}^q \gamma_k(v) \gamma_k(w) / \sqrt{\text{var}(\zeta_{ik})}$ . Then for such  $X_i(\cdot)$ , the second equation in (9) is reduced to  $X_i(v) = \sum_{k=1}^q \eta_{ik} \psi_k(v)$  with  $\{\eta_{ik}\}$  satisfying  $\text{var}(\eta_{ik}) = 1$  and  $\text{cov}(\eta_{ik}, \eta_{il}) = 0$  for any  $k \neq l$ . This, together with (11) and (12), implies that  $\beta_{jk} = 0$  in (12) for all  $j \neq k$ .

Hence, Equation (12) is reduced to

$$\begin{aligned} \xi_{ij} &= \beta_{jj}\eta_{ij} + \varepsilon_{ij} & \text{for } j = 1, \dots, r, \\ \xi_{ij} &= \varepsilon_{ij} & \text{for } j = r + 1, r + 2, \dots, \end{aligned} \quad (13)$$

that is, under the additional condition on the dimensionality of  $X_i(\cdot)$ , the curve regression (4) is reduced to  $r$  simple linear regression problems.

- (d) We provide a recap of the above results in the context of vector regression. Let  $\mathbf{y}_i$  and  $\mathbf{x}_i$  be, respectively,  $p \times 1$  and  $q \times 1$  vectors. Suppose that  $rk(\Sigma_{yx}) = r$ , where  $\Sigma_{yx} = \text{cov}(\mathbf{y}_i, \mathbf{x}_i)$ . Then the multiple linear regression problem  $\mathbf{y}_i = \mathbf{B}\mathbf{x}_i + \boldsymbol{\varepsilon}_i$  may be reduced to the  $r$  scalar linear regression problems:

$$u_{ij} = \mathbf{v}'_i \boldsymbol{\beta}_j + \varepsilon_{ij}, \quad j = 1, \dots, r. \quad (14)$$

Here,  $(u_{i1}, \dots, u_{ip})' = \mathbf{U}'\mathbf{y}_i$  and  $\mathbf{v}_i = (v_{i1}, \dots, v_{iq})' = \mathbf{V}'\mathbf{x}_i$ . Also,  $\Sigma_{yx} = \mathbf{U}\boldsymbol{\Lambda}\mathbf{V}'$  is the SVD of  $\Sigma_{yx}$  with  $\mathbf{U}\mathbf{U}' = \mathbf{I}_p$ ,  $\mathbf{V}\mathbf{V}' = \mathbf{I}_q$  and  $\boldsymbol{\Lambda}$  is a  $p \times q$  diagonal matrix with only the first  $r$  ( $\leq \min(p, q)$ ) main diagonal elements being nonzero. If  $\text{var}(\mathbf{x}_i) = \sigma^2 \mathbf{I}_q$  is satisfied in addition, Equation (14) reduces to  $r$  simple regression models  $u_{ij} = v_{ij}\beta_j + \varepsilon_{ij}$  for  $j = 1, \dots, r$ .

### 3.2 Estimation

We assume the availability of observed curves  $\{Y_i(\cdot), X_i(\cdot)\}$  for  $i = 1, \dots, n$ . Recalling  $\Sigma(u, v) = \text{cov}\{Y_i(u), X_i(v)\}$ , let

$$\widehat{\Sigma}(u, v) = \frac{1}{n} \sum_{i=1}^n \{Y_i(u) - \bar{Y}(u)\} \{X_i(v) - \bar{X}(v)\},$$

where  $\bar{Y}(u) = n^{-1} \sum_i Y_i(u)$  and  $\bar{X}(v) = n^{-1} \sum_i X_i(v)$ . Performing the SVD on  $\widehat{\Sigma}(u, v)$ , we obtain the estimators  $(\widehat{\lambda}_j, \widehat{\varphi}_j, \widehat{\psi}_j)$  for  $(\lambda_j, \varphi_j, \psi_j)$  as defined in (6). Note that this SVD is effectively an eigenanalysis of the nonnegative operator

$$\widehat{M}_1(u, u') = \int_{\mathcal{I}_2} \widehat{\Sigma}(u, v) \widehat{\Sigma}(u', v) dv, \quad (15)$$

which may be transformed into an eigenanalysis of a nonnegative definite matrix. Furthermore,  $\widehat{\varphi}_j(\cdot)$  and  $\widehat{\psi}_j(\cdot)$  may be taken as linear combinations of, respectively, the observed curves  $Y_i(\cdot)$  and  $X_i(\cdot)$ . See, for example, Section 2.2.2 of Bathia, Yao, and Ziegelmann (2010). Proposition 1 presents the asymptotic properties for the estimators  $\widehat{\lambda}_j$ . Its proof is similar to that of Theorem 1 of Bathia, Yao, and Ziegelmann (2010) and is thus omitted.

*Proposition 1.* Suppose that  $\{Y_i(\cdot), X_i(\cdot)\}$  is strictly stationary and  $\psi$ -mixing with the mixing coefficients  $\psi(k)$  satisfying the condition  $\sum_{k \geq 1} k\psi(k)^{1/2} < \infty$ . Further, assume  $\mathbb{E}\{\int_{\mathcal{I}_1} Y_i(u)^2 du + \int_{\mathcal{I}_2} X_i(v)^2 dv\}^2 < \infty$  and let  $\lambda_1 > \dots > \lambda_r > 0 = \lambda_{r+1} = \lambda_{r+2} = \dots$ . Then as  $n \rightarrow \infty$ ,

- (1)  $|\widehat{\lambda}_k - \lambda_k| = O_p(n^{-1/2})$  for  $1 \leq k \leq r$ , and
- (2)  $|\widehat{\lambda}_k| = O_p(n^{-1})$  for  $k > r$ .

We refer to Section 2.6 of Fan and Yao (2003) for further details on mixing conditions. The fast convergence for the zero-eigenvalues  $\lambda_j$  with  $j > r$  is due to the quadratic form in (15), and the relevant discussion is provided in Bathia, Yao, and Ziegelmann (2010) and Lam and Yao (2012). It follows from Proposition 1 that the ratios  $\widehat{\lambda}_{j+1}/\widehat{\lambda}_j$  for  $j < r$  are asymptotically bounded away from 0, and  $\widehat{\lambda}_{r+1}/\widehat{\lambda}_r \rightarrow 0$  in probability.

This motivates the following ratio-based estimator. In Lam and Yao (2012), a more elaborate investigation of this estimator can be found in a different context.

*The Ratio-based Estimator for the Correlation Dimension*  $r$ .  $\widehat{r} = \arg \min_{1 \leq j \leq d} \widehat{\lambda}_{j+1}/\widehat{\lambda}_j$ , where  $d > r$  is a fixed and pre-specified integer.

One alternative is to use properly defined information criteria as in, for example, Hallin and Liška (2007), where a similar idea was adopted for high-dimensional time series analysis. To this end, we define

$$\begin{aligned} \text{IC}_1(q) &= \frac{1}{d^2} \sum_{k=q+1}^d \widehat{\lambda}_k + \tau_1 q \cdot g(n), \quad \text{and} \\ \text{IC}_2(q) &= \log \left( c_* + \frac{1}{d^2} \sum_{k=q+1}^d \widehat{\lambda}_k \right) + \tau_2 q \cdot g(n), \end{aligned}$$

where  $c_*$ ,  $\tau_1$ ,  $\tau_2 > 0$  are constants,  $d > r$  is a prespecified integer, and  $g(n) > 0$  satisfies

$$n \cdot g(n) \rightarrow \infty \quad \text{and} \quad g(n) \rightarrow 0, \quad \text{as } n \rightarrow \infty. \quad (17)$$

Theorem 2 shows that  $\widehat{r} \equiv \arg \min_{0 \leq q < d} \text{IC}_i(q)$  is a consistent estimator of  $r$  for both  $i = 1, 2$ . The proof is given in the online supplementary document.

*Theorem 2.* Let the conditions of Proposition 1 hold and both  $r$  and  $d$  be fixed as  $n \rightarrow \infty$ . Then, for both  $i = 1, 2$ , we have  $P\{\text{IC}_i(r) < \text{IC}_i(q)\} \rightarrow 1$  for any  $0 \leq q < d$  and  $q \neq r$ .

The choice of  $c_*$  is not critical as it is introduced to ensure that the term inside the logarithm is positive. The proof of Theorem 2 indicates that the consistency holds for any constants  $\tau_1$  and  $\tau_2$ . However, they affect the finite sample performance of the method and therefore in practice, the choice of the tuning parameters  $\tau_1$  and  $\tau_2$  and the penalty function  $g(n)$  requires more care. In our data analysis, we set  $g(n) = n^{-1/2}$  and elaborate the choice of  $\tau_i$  using the following majority voting scheme.

We start with two values  $\tau_*$  and  $\tau^*$  such that  $\text{IC}_i(q)$  is minimized at  $q = d$  for  $\tau_i \leq \tau_*$ , and at  $q = 0$  for any  $\tau_i \geq \tau^*$ . Over the interval  $[\tau_*, \tau^*]$ , the function  $h(\tau) \equiv \arg \min_q \text{IC}_i(q)$  is non-increasing in  $\tau$ . Then, assigning a grid of values from  $[\tau_*, \tau^*]$  as  $\tau_i$ , we look for the  $q$  that is returned over the longest interval of  $\tau_i$  within  $[\tau_*, \tau^*]$ , and set such  $q$  as the estimate of  $r$ . Figure 8 shows an example of applying  $\text{IC}_2(q)$  for the selection of  $r$ , where  $\text{IC}_2(q)$  is computed over  $q = 1, \dots, 20$  for 100 different values of  $\tau_2$ . In this example,  $q = 4$  was returned most frequently as the minimizer of  $\text{IC}_2(q)$ . We have further conducted a simulation study to check whether the proposed scheme worked well on simulated datasets of varying dimensionalities, and the results have confirmed its good performance over a range of  $r$ .

### 3.3 An Illustration

We illustrate the hybrid approach by predicting the load curve on April 2, 2009, which is denoted by  $Z(\cdot)$ . Unfortunately, even after removing the long-term trend estimated in Section 2, there exist some systematic discrepancies among the profiles of daily load curves over different days in a week and different months in a year. Figure 6 shows that, while the daily loads on Tuesdays



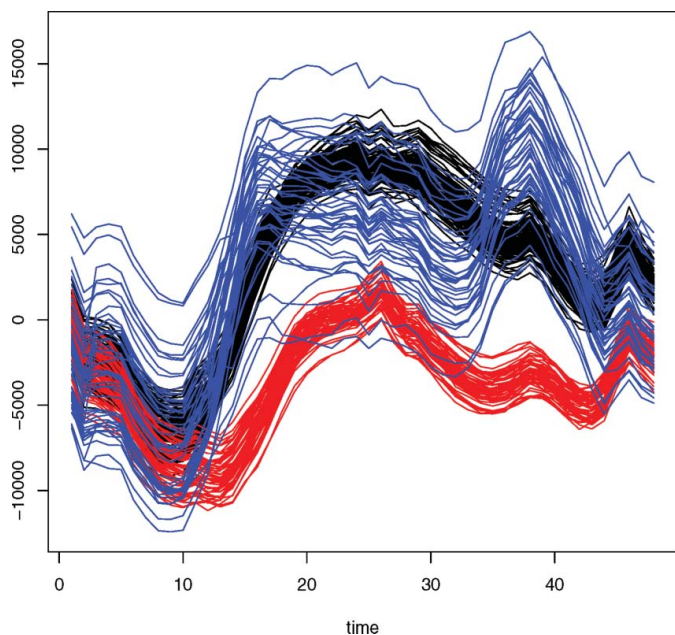


Figure 6. Detrended daily curves for Tuesdays in July (black), Saturdays in July (red), and Tuesdays in December (blue) between 1996 and 2008.

in July are similar to each other, they are distinctively different from those on Saturdays in July, and also from those on Tuesdays in December. Those profile differences are reflected predominantly in the locations and magnitudes of daily peaks.

Typically in France, daily peaks occur at noon in summer and in the evening in winter, due to the economic cycle as well as the usage of electrical heating and lighting. Hence, the daily curves and presumably their dynamic structure vary over different days within a week, and also over different months in a year; further elaboration on those features is provided in Section 4.

To forecast the load curve on Wednesday, April 2, 2009, we take the joined curve of the detrended curve on Tuesday, April 1, 2009 ( $= X^L(\cdot)$ ) and the temperature curve on April 2, 2009 ( $= X^T(\cdot)$ ) as the regressor, that is,  $X(\cdot) = (X^L(\cdot), X^T(\cdot))$ . We use all the pairs of curves on Tuesdays and Wednesdays in April from 1996 to 2008 as our observations to fit a curve regression model, and the total number of observations is  $n = 53$ . As the curves  $X_i^L(\cdot)$  range between  $-10,000$  and  $10,000$  while  $X_i^T(\cdot)$  between  $0$  and  $20$ , we apply a simple standardization step to arrange the regressor observations in the same scale. Those 53 pair curves  $\{X_i(\cdot), Y_i(\cdot)\}$  are plotted in Figure 7 together with their demeaned and standardized counterparts.

From those observations, we form a sample covariance matrix

$$\widehat{\Sigma}(u, v) = \frac{1}{53} \sum_{i=1}^{53} \{Y_i(u) - \bar{Y}(u)\} \{X_i(v) - \bar{X}(v)\}, \quad (18)$$

where  $\bar{Y}(u) = \frac{1}{53} \sum_{1 \leq i \leq 53} Y_i(u)$  is the average of all the detrended daily curves on Wednesdays in April between 1996 and 2008, and  $\bar{X}(v)$  is obtained analogously. Applying the SVD to  $\widehat{\Sigma}(u, v)$ , we obtain the estimators  $(\hat{\lambda}_k, \hat{\varphi}_k, \hat{\psi}_k)$ . To determine

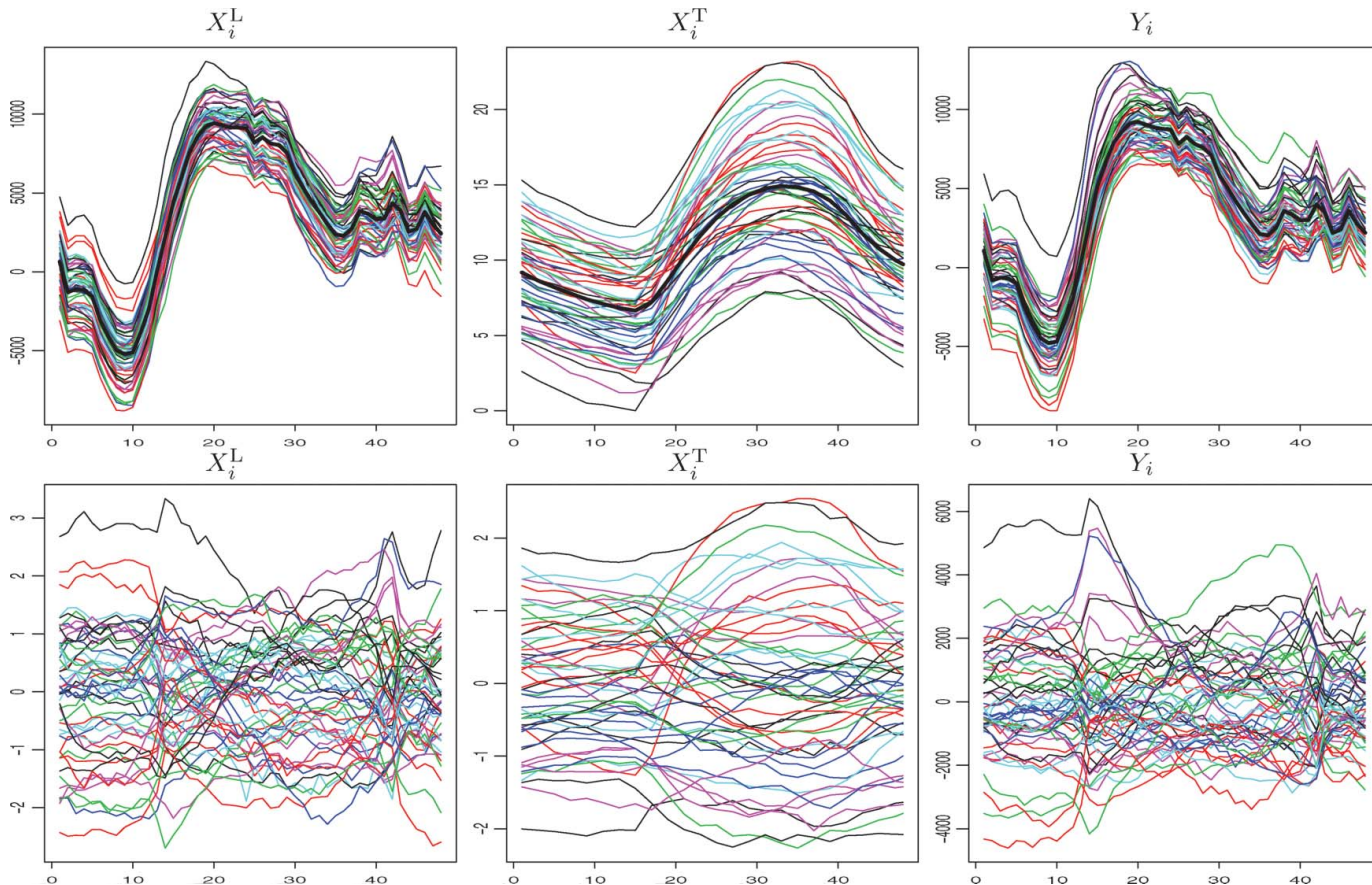


Figure 7. The 53 curves  $X_i^L(\cdot)$  (top left),  $X_i^T(\cdot)$  (top middle), and  $Y_i(\cdot)$  (top right), are plotted in the top panels along with their respective mean curves which appear in bold. The demeaned and standardized curves are plotted in the bottom panels.

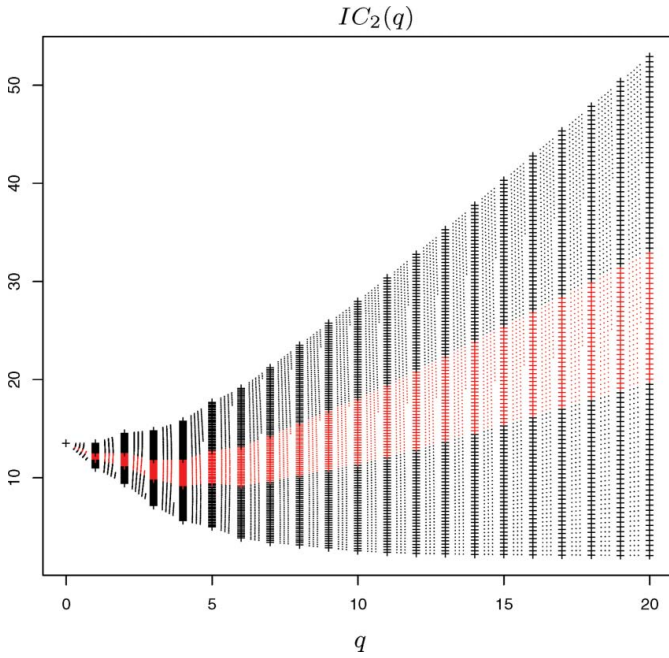


Figure 8. Plots of  $IC_2(q)$  against  $q$  for 100 different values of  $\tau_2$ . The curves with the minimum attained at  $q = 4$  are highlighted in red.

the correlation dimension, we apply the information criterion  $IC_2(q)$  with 100 different values of  $\tau_2$ , as discussed in Section 3.2. Figure 8 shows  $IC_2(q)$  against  $q$  for each of the 100  $\tau_2$ -values. With this set of data,  $q = 4$  minimizes  $IC_2(q)$  over the longest interval of  $\tau_2$ , which leads to the estimator  $\hat{r} = 4$ .

Then, our predicted load curve is of the form

$$\hat{Z}(u) = \hat{L}_w + \bar{Y}(u) + \sum_{j=1}^4 \hat{\xi}_j \hat{\varphi}_j(u), \quad (19)$$

where  $\hat{L}_w$  is the predicted weekly trend for the week containing April 2, 2009 from the GAM (3) in Section 2,  $\bar{Y}(u)$  is the mean curve as in (17), and  $\hat{\xi}_j$ ,  $j = 1, \dots, 4$  are the predictors based on linear regression models defined as follows. Based on Theorem 1, the curve linear regression  $Y_i(\cdot)$  on  $X_i(\cdot)$  may be recast into  $\hat{r} = 4$  ordinary regression models

$$\hat{\xi}_{ij} = \sum_{k=1}^{10} \beta_{jk} \hat{\eta}_{ik} + \varepsilon_{ij}, \quad i = 1, \dots, 53, \quad j = 1, \dots, 4, \quad (20)$$

where

$$\begin{aligned} \hat{\xi}_{ij} &= \int_{\mathcal{I}_1} \{Y_i(u) - \bar{Y}(u)\} \hat{\varphi}_j(u) du, \\ \hat{\eta}_{ik} &= \int_{\mathcal{I}_2} \{X_i(v) - \bar{X}(v)\} \hat{\psi}_k(v) dv, \end{aligned}$$

see (10). In (19), we choose to use the first 10 singular value components of the regressor only, as having more terms does not improve the forecasting result dramatically. Based on the least-square estimators  $\hat{\beta}_{jk}$  from the regression models (20), we obtain the predictors  $\hat{\xi}_j$  as  $\hat{\xi}_j = \sum_{k=1}^{10} \hat{\beta}_{jk} \hat{\eta}_k$ , where  $\hat{\eta}_k = \int_{\mathcal{I}_2} \{X(v) - \bar{X}(v)\} \hat{\psi}_k(v) dv$ .

We compare our method with two alternative predictors, the oracle and the baseline predictors. The oracle predictor is of the

form

$$\tilde{Z}(u) = \hat{L}_w + \bar{Y}(u) + \sum_{j=1}^4 \tilde{\xi}_j \hat{\varphi}_j(u), \quad (21)$$

which is defined similarly as our predictor (18) except with  $\hat{\xi}_j$  being replaced by  $\tilde{\xi}_j \equiv \langle Y(\cdot) - \bar{Y}(\cdot), \hat{\varphi}_j \rangle$ , where  $Y(\cdot) = Z(u) - \hat{L}_w$  denotes the detrended load curve on April 2, 2009. Since  $Y(\cdot)$  is unavailable in practice,  $\tilde{Z}(u)$  is termed as an ‘‘oracle’’ predictor. The baseline predictor is defined as

$$\bar{Z}(u) = \hat{L}_w + \bar{Y}(u), \quad (22)$$

which is the sum of the first two terms in our predictor, ignoring the dynamic dependence between days. We compare the performance of the three predictors in terms of the following two error measures

$$\begin{aligned} \text{MAPE} &= \frac{1}{48} \sum_{j=1}^{48} \left| \frac{\hat{f}_j - f_j}{f_j} \right| \quad \text{and} \\ \text{RMSE} &= \left\{ \frac{1}{48} \sum_{j=1}^{48} (\hat{f}_j - f_j)^2 \right\}^{1/2}, \end{aligned}$$

where  $\hat{f}_j$  and  $f_j$  denote the predicted and the true loads in the  $j$ th half-hour interval. The MAPE and RMSE for our predictor  $\hat{Z}(\cdot)$ , the oracle predictor  $\tilde{Z}(\cdot)$ , and the baseline predictor  $\bar{Z}(\cdot)$  are (0.91%, 634 MW), (0.60%, 420 MW), and (3.14%, 1911 MW), respectively. The three predicted curves are plotted in Figure 9 together with the true curve. Our predictor  $\hat{Z}(\cdot)$ , making good use of the dynamic dependence across different days, is a significant improvement from the baseline predictor  $\bar{Z}(\cdot)$ . While the oracle predictor  $\tilde{Z}(\cdot)$  is impractical as  $\tilde{\xi}_j$  is unavailable in practice, its superior performance in terms of both MAPE and RMSE indicates that the dimension reduction achieved via SVD retains the relevant dynamic information in the system.

We briefly discuss the extension to multistep ahead predictions using the hybrid approach, which straightforwardly translates to producing multistep ahead predictions from the GAM at the weekly level, and from the ordinary (scalar) linear regression models at the daily level. Specifically, if the corresponding week of the multistep ahead forecast is different from that of the one-step ahead forecast, the forecast is obtained by plugging the average temperature and cloud cover of the week into the fitted GAM. At the daily level modeling, the forecast of the next day’s load replaces (part of) the regressor curve to produce that of the following day, and this is repeated until the desired multistep ahead prediction is achieved. In the above example, when making a two-day ahead prediction for Thursday, April 3, 2009 on April 1, 2009, the first part of the regressor curve becomes the predicted load curve on April 2, 2009, while the second part is the daily temperature curve on April 3, 2009. The two-step ahead forecast obtained following the identical steps described in this section achieves MAPE 1.06% and RMSE 657 MW. In general, the performance of multistep ahead forecasts is worse than that of one-day-ahead forecasts as the errors in the latter are carried over to the errors in the former.

2 April 2009

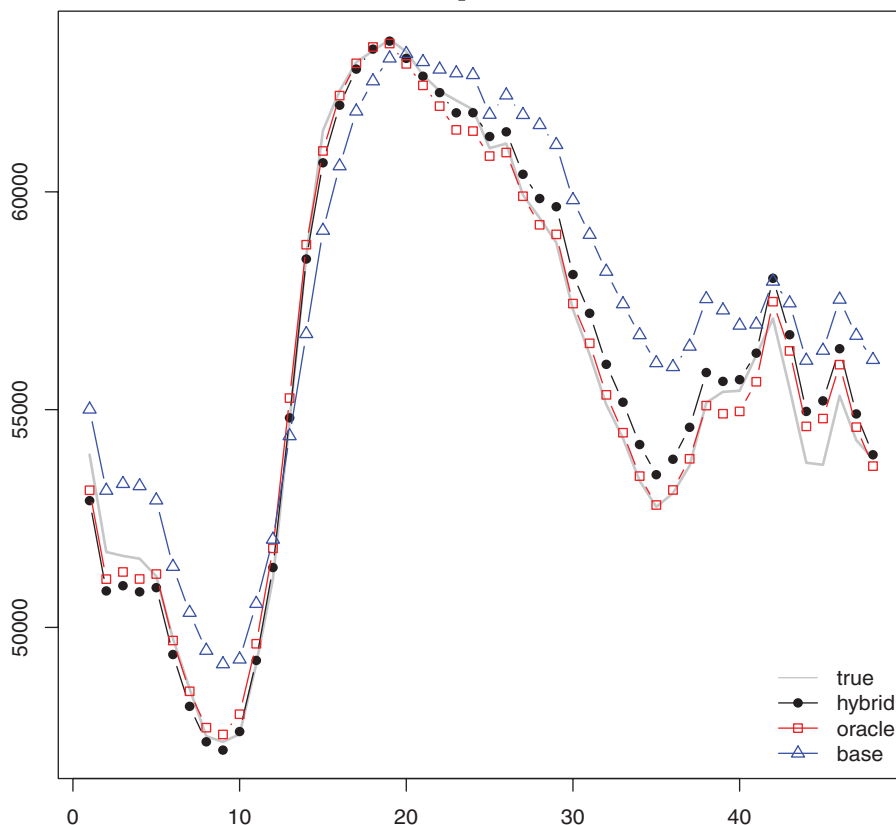


Figure 9. The true daily load curve (gray, solid) of April 2, 2009, together with its predicted curves by our method (black, filled circle), the oracle method (red, empty square), and the baseline (blue, empty triangle).

#### 4. PREDICTING DAILY LOADS IN 2009

To compare different predictive models more systematically, and to gain further appreciation of the performance of our method over different periods of a year, we predict the daily load curves for all days in 2009. For each day in 2009, we used the data from January 1, 1996 to its previous day to build the prediction models in the same manner as described in Section 3.3, that is, first the trend component (i.e., as  $\hat{L}_w$  in (19)) is predicted by the GAM model in (3), and then the residual process is divided into daily curves for curve linear regression.

##### 4.1 Classification of Daily Curves

Discussions in Section 3.3 indicate that we need to treat the daily residual curves on each day of a week differently. For the French electricity load dataset, we are furnished with the *day type* of each day, which is a classification of the daily curves determined by the experts at EDF. The day type is defined with respect to different days of a week, and bank holidays are assigned to separate day types according to their profiles. See Table 1 for the summary of day types. Furthermore, to take into

account the seasonal changes which may be present in the shapes ( $\mathbb{E}\{Y_i(\cdot)\}$  and  $\mathbb{E}\{X_i(\cdot)\}$ ) as well as the dependence structure ( $\Sigma(u, v) = \text{cov}(Y_i(u), X_i(v))$ ) of daily curves, we divide 1 year into nine seasonal segments: January to February, March, April, May, June to July, August to September, October, November, and December. This segmentation was determined by inspecting the decomposition of electricity loads with respect to adaptively chosen orthonormal functions. More precisely, we performed principal component analysis on the pool of demeaned daily curves (according to the day type), and decomposed them with respect to the first principal direction. By examining the changes in the decomposition over a year (see Figure 10), we obtained the segmentation of a year as provided above.

While the above classification lacks a rigorous statistical foundation, the prediction model based on this classification performs well in practice. Besides, classification of electricity load curves can stand alone as an independent research problem which has attracted considerable attention, see, for example, Chiou and Li (2007), Ray and Mallick (2006), Serban and Wasserman (2005), and James and Sugar (2003) for functional clustering, and Antoniadis et al. (2010) in the context of

Table 1. Day types furnished by the EDF experts

Index	0	1	2	3	4	5	6	7
Day type	Mon	Tue–Thu	Fri	Sat	Sun (rest)	Sun (Jun–Jul)	Sun (Aug)	Sun (Dec)

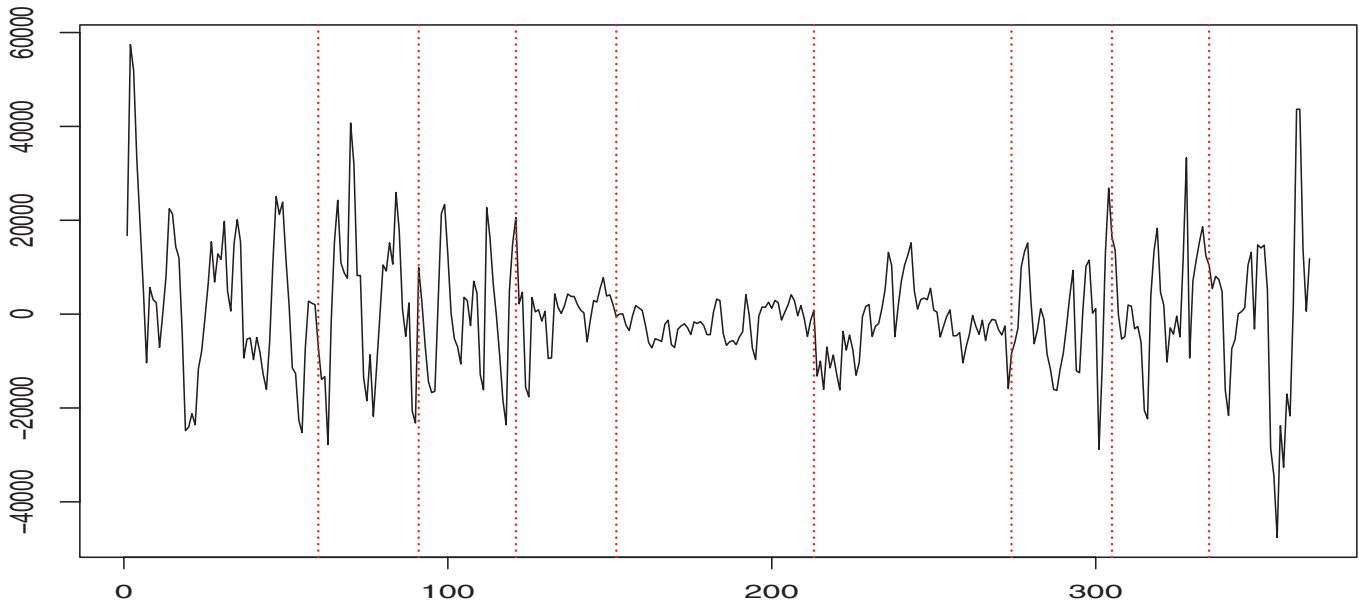


Figure 10. Decomposition of the daily curves from 2008 with respect to the first principal component estimated from the pooled daily curves between 1996 and 2008: seasonal segments are denoted by dotted, red lines. The online version of this figure is in color.

electricity loads classification. In summary, each daily curve is classified according to the day of a week and the season of a year, and there are 67 pairs of classes for any two consecutive days between 1996 and 2009. For each pair of classes, we fit a prediction model separately in the same manner as described in Section 3.3.

#### 4.2 Prediction Comparisons

In applying the proposed hybrid method, we consider four different versions H1–H4 depending on the choice of regressor. H1 uses the load curve on the current day as the regressor (i.e.,  $X(\cdot) = X^L(\cdot)$ ). H2 uses the joined curve of the load curve on the current day and the temperature curve on the next day (i.e.,  $X(\cdot) = (X^L(\cdot), X^T(\cdot))$ ), as demonstrated in Section 3.3. H3 adopts the same regressor as H1 but with a half-day curve such that, if we are forecasting the electricity load from 00:30 to 12:00 on the next day, the load curve on the current day from 12:30 to 24:00 is used as the regressor curve; when forecasting the curve from 12:30 to 24:00, the regressor curve is the load curve from 00:30 to 12:00 on the same day. Similarly, H4 employs the same regressor as H2 but also with half-day curves. To facilitate a more comprehensive comparison, we predict the daily load curves by our proposed hybrid method (19), the oracle method (21), and the baseline method (22). We also include in the comparison study, the prediction results from the EDF operational model, the SARIMA model as in Taylor and McSharry (2008), a combination of the GAM and SARIMA (GSARIMA) methods, and the exponential smoothing technique (EST) discussed in Taylor (2010). In total, there are 10 different models used in our comparison study.

Denote the number of observations for each pair of classes by  $n$ . Since we impose an upper bound of 10 on the correlation dimension  $r$ , we choose to include only those classes with  $n$  greater than 15 in our comparison study. Also, only the first 10  $\eta_{ik}$ 's are used in the scalar linear regression models (12), as

having more than 10 terms does not improve the results dramatically while  $n$  is allowed to be as small as 15. We further note that it is considered a more challenging task to forecast electricity loads for holidays than those for working days, and often additional prior information is used for holidays in practice. Instead of making the whole exposition overcomplicated, we focus on the forecasting for the working days only. There are 315 days in total where all the conditions stated above are satisfied. Note that in the hybrid approach, we require the forecasts of the average temperature of the following week, as well as the temperature curve of the next day. As such information can easily be furnished by Météo-France for this particular dataset, we may assume that the forecast of the next day's temperature has been provided in the form of a curve, and the weekly average temperature of the following week can be replaced by the mean of such a forecast (in accordance with the assumption that the long-term trend varies little within each week). Since the resulting MAPE (1.38%) and RMSE (891 MW) from (H2) with the predicted temperature values are only slightly worse than those obtained with the true temperature values (MAPE 1.35%, RMSE 869 MW), we report in what follows the results obtained assuming that all such necessary information is available. Forecasting errors measured by the MAPE and RMSE are summarized in Table 2, and we also present the errors with respect to different seasons and day types in Figures 11 and 12.

The prediction based on any model considered is more accurate in summer than in winter, see Figure 11. The relative difficulty of load forecasting in winter has been noted for the French dataset in Dordonnat et al. (2008), Dordonnat et al. (2011), and Cugliari (2011). SARIMA and GSARIMA are consistently outperformed by other methods by a large margin, and between the two, GSARIMA achieves smaller forecasting errors. Between H1 (H3) and H2 (H4), the latter attains considerably smaller forecasting errors as it makes use of more information on the temperature, although Figure 11 shows that this observation is

Table 2. Summary of MAPE and RMSE of the electricity load forecasts for January 1, 2009–December 31, 2009 from our hybrid modeling (H1, H2, H3, H4), oracle, base, SARIMA, GSARIMA, EST, and operational model

	H1	H2	H3	H4	Oracle	Base	SARIMA	GSARIMA	EST	Operation
MAPE (%)	1.54	1.35	1.37	1.20	0.46	3.05	2.55	2.49	1.97	0.93
RMSE (MW)	1018	869	918	787	317	1882	1607	1586	1330	625

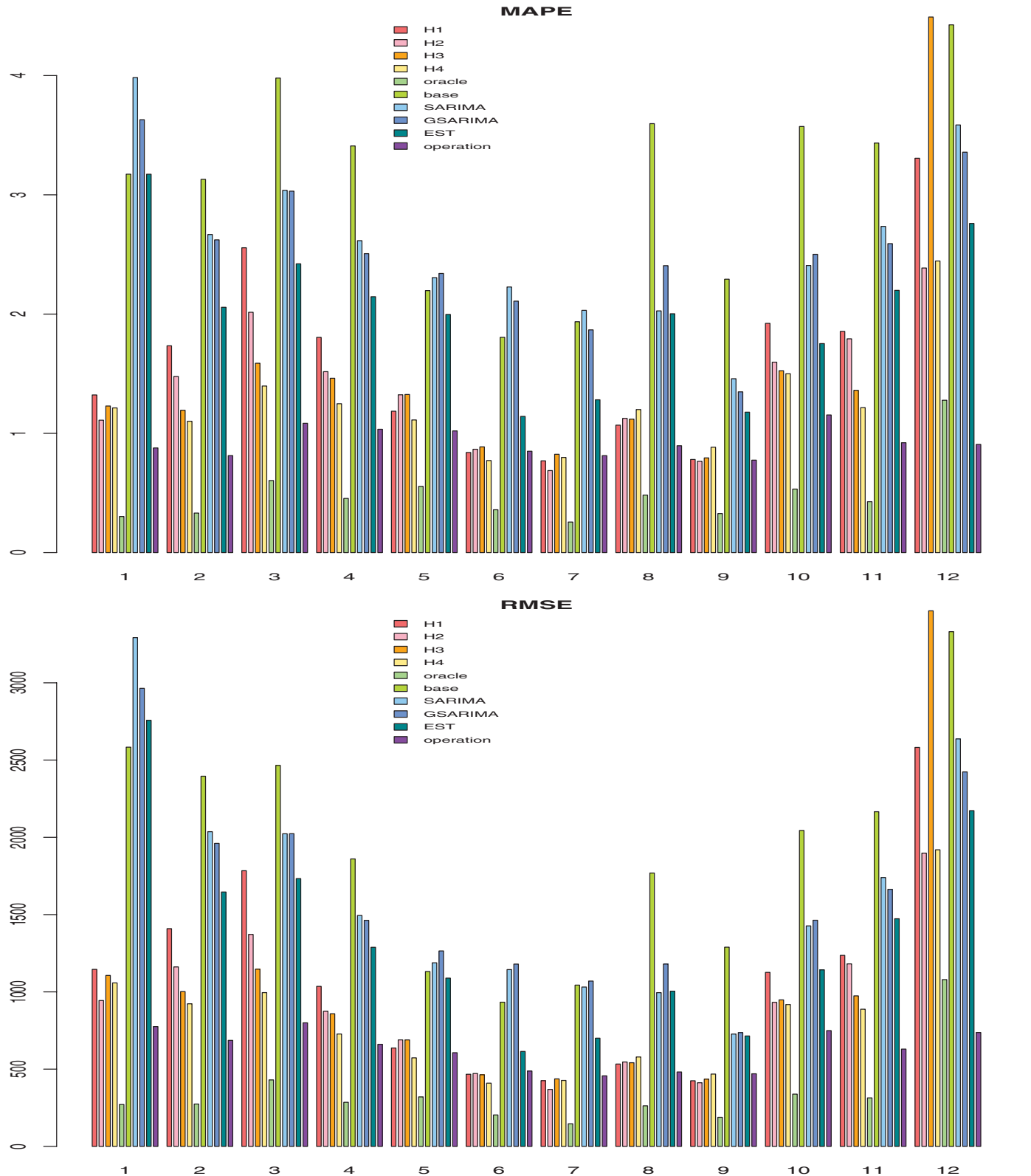


Figure 11. Bar plots of MAPE (top) and RMSE (bottom) with respect to months.

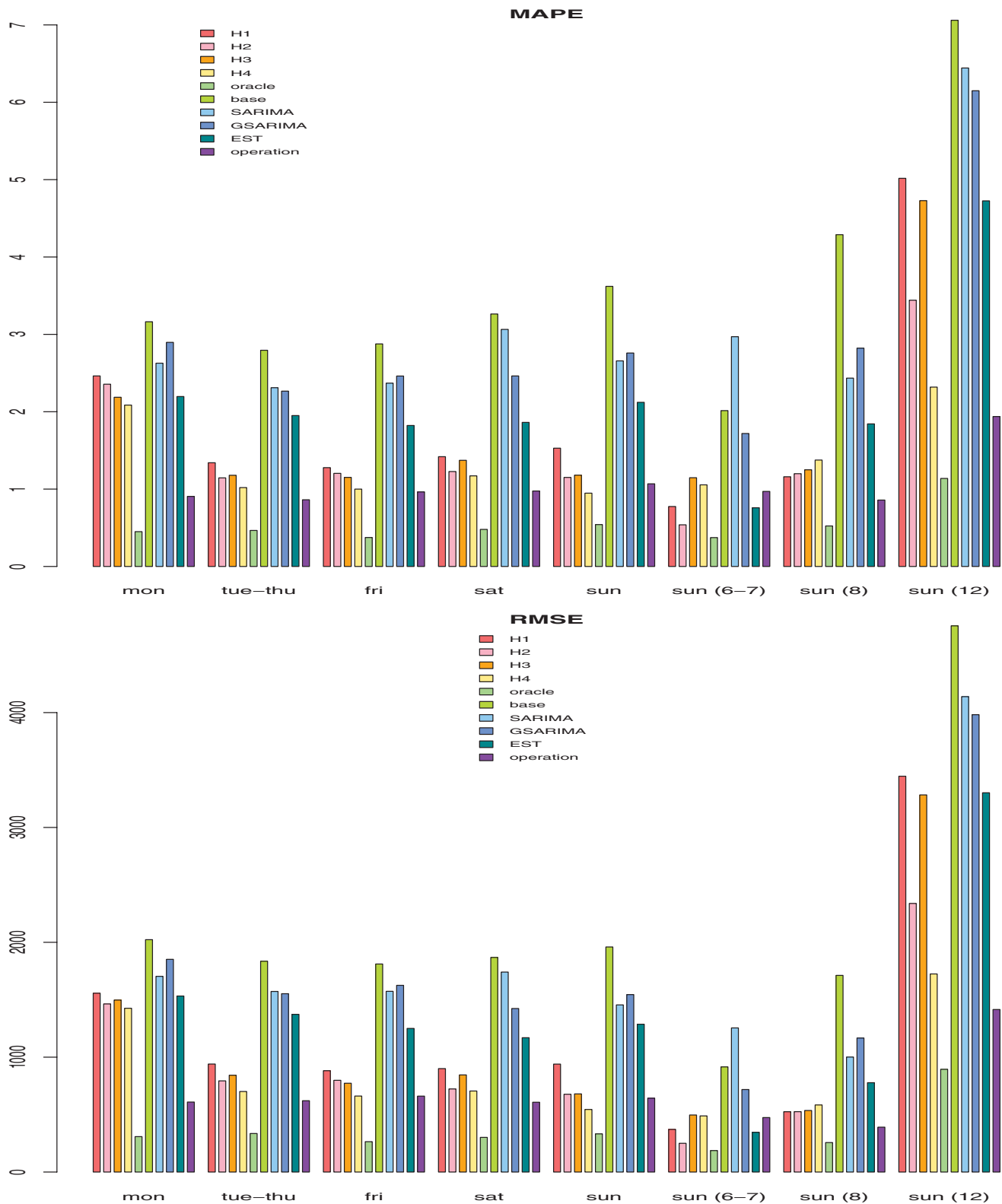


Figure 12. Bar plots of MAPE (top) and RMSE (bottom) with respect to the day type determined by experts; from left to right: Mondays, Tuesdays–Thursdays, Fridays, Saturdays, Sundays (except for June–August and December), Sundays in June and July, Sundays in August, and Sundays in December.

not held consistently throughout the year. We note that the performance of our approach may further be improved by making an adaptive choice of regressor curve dependent on the level of temperature.

From Figure 11, it is interesting to observe that the half-day-based approaches, H3 or H4, achieve better forecasting performance than H1 or H2 in some colder months (February–April, October–November), while the opposite is true in warmer

months. This may be understood in relation with the variability among the curves, which is considerably greater in winter than in summer (see, e.g., Figure 6). On a similar note, while forecasting errors from the EDF operational model are smaller than those from hybrid approaches on average, the difference is noticeably reduced from May to September. Indeed, H1 and H2 return errors that are comparable to or even smaller than those from the operational model in June, July, and September. In terms of day type, the forecasting errors from the hybrid methods are larger on Mondays than for the rest of a week on average (see Figure 12), which may also be due to the greater variability in the relationship between the curves from Sundays and Mondays. The oracle predictor attains the minimum errors throughout the year except for in December, which suggests that there is a scope for improvement in the hybrid approach by improving the linear regression fit at the daily level.

There are certain factors that are known to have substantial influence on daily electricity loads yet have not been incorporated into our hybrid modeling. For example, from November to March, EDF offers special tariff days to large businesses as financial incentives, which are activated to cut heavy electricity consumption in winter. Since the scheme is known to affect not only the daily loads on the special tariff days but also on the days before and after those days, we expect that including prior information on such days, for example, by creating new classes, can further improve the quality of the forecasts especially in winter.

## 5. CONCLUSIONS

In this article, we proposed a hybrid approach to electricity load modeling with the aim of forecasting daily electricity loads. In the hybrid procedure, we model the overall and seasonal trends of the electricity load data at the weekly level, by fitting a GAM with temporal and meteorological factors as explanatory variables. At the daily level, the serial dependence among the daily load curves is modeled under the assumption that the curves from two successive days have a linear relationship, and we propose a framework that effectively reduces the curve linear regression to a finite number of scalar linear regression problems. To the best of our knowledge, it has not been explored elsewhere how to model the multilayered features of an electricity load dataset at multiple levels separately. Compared with the current operational model at EDF, our proposed method is more model-centered and developed without much of a specific knowledge that has been included in the former, while it still retains a competitive prediction capacity. We also note that our approach has the potential to be more adaptive to the changing electricity consumption environment, as well as being applicable to a wider range of problems without much human intervention.

When applying the hybrid approach to the real-life dataset in Section 4.2, some factors which may have substantial influence over daily electricity loads have not been fully exploited. This could have resulted in worsening the performance of our method for winter days when compared with the operational model, and it remains as a task to incorporate such relevant information into our method for practical applications. Also, as briefly mentioned in Section 4.2, an adaptive choice of the regressor

curve, depending, for example, on the level of temperature, may lead to better results in daily load forecasting. Indeed, an automatic selection of the regressor in the curve linear regression framework may benefit the prediction performance as a generic tool beyond electricity load forecasting, and we leave the problem for future research.

## SUPPLEMENTARY MATERIALS

The supplementary document includes the proofs of Theorems 1–2.

[Received January 2012. Revised May 2012.]

## REFERENCES

- Antoniadis, A., Brossat, X., Cugliari, J., and Poggi, J. M. (2010), "Functional Clustering using Wavelets," in *Proceedings of the Nineteenth International Conference on Computational Statistics (COMPSTAT)*, Paris, France, August 22–27, pp. 697–704. [16]
- Antoniadis, A., Paparoditis, E., and Sapatinas, T. (2006), "A Functional Wavelet Kernel Approach for Time Series Prediction," *Journal of the Royal Statistical Society, Series B*, 68, 837–857. [8]
- Bathia, N., Yao, Q., and Ziegelmann, F. (2010), "Identifying the Finite Dimensionality of Curve Time Series," *The Annals of Statistics*, 38, 3352–3386. [12,13]
- Bunn, D. W., and Farmer, E. D. (1985), *Comparative Models for Electrical Load Forecasting*, New York: Wiley. [8]
- Chiou, J. M., and Li, P. L. (2007), "Functional Clustering and Identifying Substructures of Longitudinal Data," *Journal of the Royal Statistical Society, Series B*, 69, 679–699. [16]
- Chiou, J. M., Müller, H. G., and Wang, J. L. (2004), "Functional Response Models," *Statistica Sinica*, 14, 659–677. [11]
- Cottet, R., and Smith, M. (2003), "Bayesian Modeling and Forecasting of Intraday Electricity Load," *Journal of the American Statistical Association*, 98, 839–849. [8]
- Cugliari, J. (2011), "Prévision non paramétrique de processus à valeurs fonctionnelles: Application à la consommation d'électricité," Ph.D. dissertation, Université Paris Sud. [8,17]
- Cupidon, J., Eubank, R., Gilliam, D., and Ruyngaert, F. (2008), "Some Properties of Canonical Correlations and Variates in Infinite Dimensions," *Journal of Multivariate Analysis*, 99, 1083–1104. [11]
- Dordonnat, V., Koopman, S. J., Ooms, M., Dessertaine, A., and Collet, J. (2008), "An Hourly Periodic State Space Model for Modelling French National Electricity Load," *International Journal of Forecasting*, 24, 566–587. [8,17]
- (2011), "Dynamic Factors in Periodic Time-Varying Regressions With an Application to Hourly Electricity Load Modelling," *Computational Statistics and Data Analysis*, 56, 3134–3152. [8,17]
- Engle, R. F., Granger, C. W. J., Rice, J., and Weiss, A. (1986), "Semiparametric Estimates of the Relation Between Weather and Electricity Sales," *Journal of the American Statistical Association*, 81, 310–320. [7,8]
- Eubank, R., and Hsing, T. (2008), "Canonical Correlation for Stochastic Processes," *Stochastic Processes and their Applications*, 118, 1634–1661. [11]
- Fan, J., and Yao, Q. (2003), *Nonlinear Time Series*, New York: Springer. [13]
- Fan, J., and Zhang, J. T. (1998), "Functional Linear Models for Longitudinal Data," *Journal of the Royal Statistical Society, Series B*, 39, 254–261. [11]
- Fan, S., and Hyndman, R. J. (2012), "Short-Term Load Forecasting Based on a Semi-Parametric Additive Model," *IEEE Transactions on Power Systems*, 27, 134–141. [8]
- Hall, P., and Horowitz, J. L. (2007), "Methodology and Convergence Rates for Functional Linear Regression," *The Annals of Statistics*, 35, 70–91. [11]
- Hall, P., and Vial, C. (2006), "Assessing the Finite Dimensionality of Functional Data," *Journal of the Royal Statistical Society, Series B*, 68, 689–705. [12]
- Hallin, M., and Liška, R. (2007), "Determining the Number of Factors in the General Dynamic Factor Model," *Journal of the American Statistical Association*, 102, 603–617. [13]
- Hannan, E. J. (1961), "The General Theory of Canonical Correlation and its Relation to Functional Analysis," *Journal of the Australian Mathematical Society*, 2, 229–242. [11]

- Harvey, A., and Koopman, S. (1993), "Forecasting Hourly Electricity Demand Using Time-Varying Splines," *Journal of the American Statistical Association*, 88, 1228–1253. [8]
- Hastie, T. J., and Tibshirani, R. J. (1990), *Generalized Additive Models*, Chapman & Hall/CRC. [8]
- He, G., Müller, H. G., and Wang, J. L. (2000), "Extending Correlation and Regression From Multivariate to Functional Data," in *Asymptotics in Statistics and Probability*, ed. M. Puri, VSP: Leiden, pp. 197–210. [11]
- (2003), "Functional Canonical Analysis for Square Integrable Stochastic Processes," *Journal of Multivariate Analysis*, 85, 54–77. [11]
- Hyndman, R. J., Koehler, A. B., Snyder, R. D., and Grose, S. (2002), "A State Space Framework for Automatic Forecasting Using Exponential Smoothing Methods," *International Journal of Forecasting*, 18, 439–454. [8]
- James, G. M., and Sugar, C. A. (2003), "Clustering for Sparsely Sampled Functional Data," *Journal of the American Statistical Association*, 98, 397–408. [16]
- Lam, C., and Yao, Q. (2012), "Factor Modelling for High-Dimensional Time Series: Inference for the Number of Factors," *The Annals of Statistics*, 40, 694–726. [13]
- Pierrot, A., and Goude, Y. (2011), "Short-Term Electricity Load Forecasting With Generalized Additive Models," in *Proceedings of ISAP power 2011*, pp. 410–416. [8]
- Pierrot, A., Lалуque, N., and Goude, Y. (2009), "Short-Term Electricity Load Forecasting With Generalized Additive Models," in *Proceedings of the Third International Conference on Computational and Financial Econometrics (CFE)*, p. 9. [8]
- Ramanathan, R., Engle, R., Granger, C. W. J., Vahid-Araghi, F., and Brace, C. (1997), "Short-Run Forecasts of Electricity Loads and Peaks," *International Journal of Forecasting*, 13, 161–174. [8]
- Ramsay, J. O., and Dalzell, C. J. (1991), "Some Tools for Functional Data Analysis (with discussions)," *Journal of the Royal Statistical Society, Series B*, 53, 539–572. [11]
- Ray, S., and Mallick, B. (2006), "Functional Clustering by Bayesian Wavelet Methods," *Journal of the Royal Statistical Society, Series B*, 68, 305–332. [16]
- Serban, N., and Wasserman, L. (2005), "CATS: Clustering After Transformation and Smoothing," *Journal of the American Statistical Association*, 100, 990–999. [16]
- Silverman, B. W. (1996), "Smoothed Functional Principal Components Analysis by Choice of Norm," *The Annals of Statistics*, 24, 1–24. [11]
- Smithies, F. (1937), "The Eigenvalues and Singular Values of Integral Equations," in *Proceedings of the London Mathematical Society*, pp. 255–279. [12]
- Taylor, J. W. (2010), "Triple Seasonal Methods for Short-Term Electricity Demand Forecasting," *European Journal of Operational Research*, 204, 139–152. [8,17]
- Taylor, J. W., and Buizza, R. (2002), "Neural Network Load Forecasting With Weather Ensemble Predictions," *IEEE Transactions on Power Systems*, 17, 626–632. [7]
- Taylor, J. W., de Menezes, L. M., and McSharry, P. E. (2006), "A Comparison of Univariate Methods for Fore-Casting Electricity Demand up to a Day Ahead," *International Journal of Forecasting*, 22, 1–16. [8]
- Taylor, J. W., and McSharry, P. E. (2008), "Short-Term Load Forecasting Methods: An Evaluation Based on European Data," *IEEE Transactions on Power Systems*, 22, 2213–2219. [7,17]
- Wood, S. N. (2004), "Stable and Efficient Multiple Smoothing Parameter Estimation for Generalized Additive Models," *Journal of the American Statistical Association*, 99, 673–686. [9]
- (2006), *Generalized Additive Models: An Introduction With R*, London: Chapman and Hall/CRC Press. [8,9]
- (2011), "Fast Stable Restricted Maximum Likelihood and Marginal Likelihood Estimation of Semiparametric Generalized Linear Models," *Journal of the Royal Statistical Society, Series B*, 73, 3–36. [9]
- Yang, W., Müller, H. G., and Stadtmüller, U. (2011), "Functional Singular Component Analysis," *Journal of the Royal Statistical Society, Series B*, 73, 303–324. [11]
- Yao, F., Müller, H. G., and Wang, J. L. (2005), "Functional Data Analysis for Sparse Longitudinal Data," *Journal of the American Statistical Association*, 100, 577–590. [11]